Current Problems in Diagnostic Radiology ▮ (2016) ▮▮▮–▮▮▮

Current Problems in Diagnostic Radiology

journal homepage: www.cpdrjournal.com

Sorting the Alphabet Soup of Renal Pathology: A Review

Sheilah M. Curran-Melendez, MD[a,*], Matthew S. Hartman, MD[a], Matthew T. Heller, MD[b], Nancy Okechukwu, MD[a]

[a] Department of Radiology, Allegheny General Hospital, Allegheny Health Network, Pittsburgh, PA
[b] University of Pittsburgh Medical Center, Department of Radiology, Pittsburgh, PA

Diseases of the kidney often have their names shortened, creating an arcane set of acronyms which can be confusing to both radiologists and clinicians. This review of renal pathology aims to explain some of the most commonly used acronyms within the field. For each entity, a summary of the clinical features, pathophysiology, and radiological findings is included to aid in the understanding and differentiation of these entities. Discussed topics include acute cortical necrosis, autosomal dominant polycystic kidney disease, angiomyolipoma, autosomal recessive polycystic kidney disease, acute tubular necrosis, localized cystic renal disease, multicystic dysplastic kidney, multilocular cystic nephroma, multilocular cystic renal cell carcinoma, medullary sponge kidney, paroxysmal nocturnal hemoglobinuria, renal papillary necrosis, transitional cell carcinoma, and xanthogranulomatous pyelonephritis.

Introduction

Diseases of the kidney often have their names shortened, creating an arcane set of acronyms that can be confusing to both radiologists and clinicians. This review of renal pathology aims to explain some of the most commonly used acronyms within the field. For each entity, a summary of the clinical features, pathology, and radiological findings is included.

Acute Cortical Necrosis

Clinical Features

Acute cortical necrosis (ACN) is a rare cause of acute renal failure, accounting for 2% of cases in adults.[1] It is most common in pregnant or postpartum women, who represent 50%-60% of these cases,[2] but is also found in neonates; approximately 10% of cases occur in children. Common causes of ACN include sepsis, abruptio placentae, intrauterine fetal death, uterine hemorrhage, renal vein thrombosis, dehydration, fetomaternal transfusion, severe hemolytic anemia, hemolytic-uremic syndrome, nephrotoxic contrast agents, certain medications (eg, nonsteroidal anti-inflammatory drugs) and trauma. Patients present with abdominal or costovertebral tenderness, hypotension, and tachycardia. Treatment is largely supportive, with goals of gaining and maintaining hemodynamic stability, start of early dialysis, and treatment of underlying etiologies.

Pathology

The underlying pathophysiology of ACN is poorly understood, but it involves ischemic injury to the renal cortex, primarily the renal tubules, because of arterial insufficiency. The renal medulla and papilla are spared because of lower oxygen tension in this portion of the kidney. Most underlying etiologies cause bilateral ACN, but unilateral root causes exist, such as renal vein thrombosis. ACN is almost always diffuse, although focal ACN has been described. Kidneys may be normal in size or mildly enlarged, with foci of hemorrhage or necrosis involving the cortex.

Radiologic Findings

Cross-sectional imaging of the kidneys reveals mild enlargement of both the kidneys. On ultrasound, the kidneys are diffusely hyperechoic relative to renal parenchyma with loss of the normal corticomedullary differentiation. Unenhanced computed tomography (CT) evaluation of ACN demonstrates hyperdensity of the renal cortex with hypodense renal medulla. On enhanced CT, there is hypoattenuation of the renal cortex with normal enhancement of the renal medulla (Fig 1). A subcapsular rim of normally enhancing tissue may be identified, representing vascularization by capsular vessels. Both T1-weighted and T2-weighted magnetic resonance imaging (MRI) shows hypointensity of the renal cortex and columns of Bertin, and a thin, subcapsular rim of hyperintensity which may be identified on T2-weighted images. Patients who recover from ACN often have decreased renal size, with calcification of the renal cortex at the site of cortical necrosis visible both on CT and radiographs. When these calcifications involve both the inner and outer aspect of the cortex, the classic “tramline” sign may be seen.

* Reprint requests: Sheilah M. Curran-Melendez, Department of Radiology, Allegheny General Hospital, Allegheny Health Network, 320 E, North Ave, Pittsburgh, PA 15212.
E-mail address: sheilah.curran@gmail.com (S.M. Curran-Melendez).

http://dx.doi.org/10.1067/j.cpradiol.2016.01.003
0363-0188/

Fig. 1. Acute cortical necrosis. Axial contrast-enhanced CT image shows a low-density zone of cortical necrosis (black arrows) with a thin subcapsular rim of enhancing tissue (white arrows), which is vascularized by capsular vessels and should not be confused with adequate perfusion.

Autosomal Dominant Polycystic Kidney Disease

Clinical Features

Autosomal dominant polycystic kidney disease (ADPKD) is an inherited disorder, characterized by the formation of cysts within the kidney, but also in other organs such as the liver, pancreas, and seminal vesicles. Additional abnormalities have also been identified with this disorder, such as heart valve defects, intracranial and aortic aneurysms, and abdominal wall hernias. ADPKD has an incidence of 1 in 400 births and affects approximately 400,000 people in the United States.[3] Patients with ADPKD are often asymptomatic until adulthood (mean age of onset of end-stage disease is 54.3 years)[3] when they present with symptoms of renal functional decline.

Pathology

Current theory is that the underlying pathophysiology of ADPKD hinges on dysfunction of primary cilia, because of abnormalities in the PKD1 and PKD2 genes, which encode the polycistin-1 and polycystin-2 proteins, respectively.[4] Abnormalities in these proteins lead to increased epithelial proliferation and fluid secretion, which contribute to the formation of multiple cysts. As cysts enlarge, they cause vascular compromise, leading to renal ischemia and activation of the renal-angiotensin-aldosterone system. This in turn leads to cyst expansion and worsening of vascular compromise—a negative feedback loop. Gross evaluation of renal specimens reveals markedly enlarged kidneys, with a bosselated surface formed by innumerable renal cysts (Fig 2).

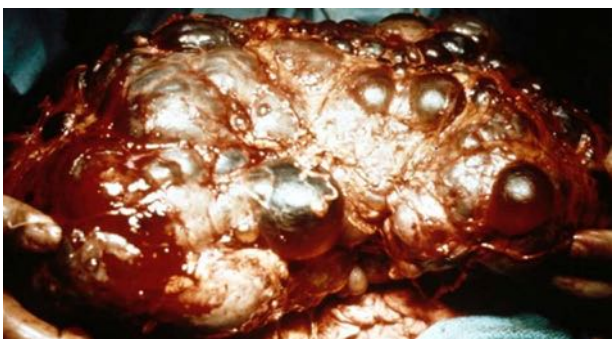

Fig. 2. Autosomal dominant polycystic kidney disease. Gross specimen demonstrating an enlarged kidney with a bosselated contour composed of subcapsular cysts. (Color version of figure is available online.)

Radiologic Findings

Cross-sectional imaging shows bilateral massively enlarged kidneys with a tremendous number of cysts, which may be complicated (containing proteinaceous or hemorrhagic fluid) or simple in appearance. On ultrasound, simple cysts are anechoic with very thin walls, whereas complicated cysts often contain echogenic material and may have wall calcifications. On CT, simple cysts have thin walls, with internal contents measuring near water attenuation, whereas complicated cysts are often hyperdense and may feature thin septations (Fig 3). On MRI, simple cysts are T1 hypointense and T2 hyperintense. Complicated cysts are more varied in signal characteristic, but most are usually T1 hyperintense because of internal proteinaceous material, whereas T2 signal characteristics are variable. On enhanced imaging (either CT or MRI), cysts may show a thin rim of wall enhancement. If foci of solid enhancement or thick septal enhancement are identified within a cyst, renal cell carcinoma (RCC) should be considered. Patients with ADPKD do not have an increased risk of RCC, although when diagnosed in a patient with ADPKD, RCC is bilateral in 12% of cases.[5]

Angiomyolipoma

Clinical Features

Renal angiomyolipomas (AMLs) are the most common benign tumors of the kidney and are derived from perivascular epithelial cells. Their overall prevalence is 2.2% in the general population, but may be as high as 45%-80% in patients with tuberous sclerosis.[6] There is a 4:1 female-to-male predilection, with most AMLs diagnosed in middle-aged women.[7]

Pathology

AMLs are benign mesenchymal tumors composed of vascular, adipose, and immature smooth muscle cells. Although the origin of these lesions is contested, the most widely accepted theory suggests that these benign tumors originate from metaplastic change of the reticuloendothelial cells of capillaries in response to stimuli.[8] On gross pathology, AMLs appear as a mixture of gray-white, red, and yellow material representing a combination of muscular, vascular, and adipose tissue. Although the tumor is benign, there may be visible invasion of local structures, including lymph nodes, renal veins, and the renal capsule.

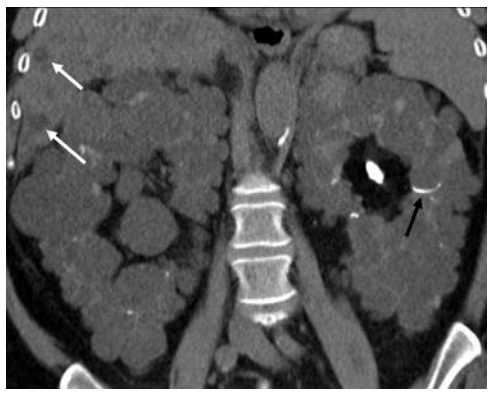

Fig. 3. Autosomal dominant polycystic kidney disease. Coronal unenhanced CT image shows enlarged kidneys with innumerable cysts replacing the renal parenchyma. Some cysts demonstrate thin peripheral calcifications (black arrow). Cysts are also present within the liver (white arrows).

Fig. 4. Angiomyolipoma. Sagittal ultrasound image of the left kidney shows a hyperechoic mass (arrow) arising from the lower pole of the kidney.

Radiologic Findings

AMLs are often radiographically diagnosed by the presence of macroscopic fat within the lesion. On ultrasound, AMLs appear as hyperechoic masses relative to surrounding renal parenchyma (Fig 4). As RCC may have a similar sonographic appearance, ultrasound characteristics are often insufficient for the diagnosis of AML, and further evaluation with CT or MRI is generally needed. Macroscopic fat within an AML demonstrates Hounsfield units of less than −20 on CT (Fig 5). Often, this is sufficient for diagnosis. Enhancement characteristics are variable, as they are based on the level of vascular tissue within the lesion. Rarely, aneurysms may be identified internally. MRI for evaluation of macroscopic fat is best performed with fat saturation techniques, allowing detection of macroscopic fat as signal dropout between pre–fat saturated images and post–fat saturated images. In-phase and out-of-phase magnetic resonance sequences may also be employed for the diagnosis of AML. In these cases, the interface between renal parenchyma and fat demonstrates the so-called "India ink" artifact, confirming the presence of fat within the lesion. In the rare case of a lipid-poor AML, CT, and MRI are often insufficient for differentiation between AML and RCC. Surgical excision is required for diagnosis in these cases. Additionally, the presence of internal calcifications, which are not associated with AMLs, should increase suspicion for RCC and such lesions should also be surgically excised.

Autosomal Recessive Polycystic Kidney Disease

Clinical Features

Autosomal recessive polycystic kidney disease (ARPKD) is estimated to occur in 1 out of every 20,000 live births.[9] Initial presentation of ARPKD is highly age dependent, with renal complications prominent in younger patients, and hepatic dysfunction in older patients.

Pathology

ARPKD is characterized by a mutation of the PKHD1 gene. PKHD1 encodes fibrocystin, an integral membrane protein found in renal collecting ducts and the epithelial cells of hepatic bile ducts.[10] Defects in this protein lead to dysfunction of the renal and hepatic cilia, which predisposes the patient to renal cyst formation and hepatic fibrosis. On gross pathology, kidneys in patients with ARPKD are symmetrically enlarged, with a large number of small cystic spaces (Fig 6A) involving the renal cortex and medulla. These spaces represent ectatic collecting tubules. These dilated cystic tubules often obliterate the corticomedullary junction, making corticomedullary differentiation impossible (Fig 6B).

Radiologic Findings

Sonographic assessment shows the kidneys to be symmetrically enlarged and diffusely hyperechoic with a thin hypoechoic rim representing the renal cortex (Fig 7). Prenatally, this appearance may not be present until the second trimester. Rarely, small discrete parenchymal cysts may be visible. On CT, the enlarged kidneys are low in attenuation and may better reveal cystic changes. If contrast agent is given in a patient with preserved renal function, a striated pattern of renal cortical excretion is seen due to accumulation of contrast agent within dilated tubules (Fig 8). In those patients with depressed renal function who receive contrast agent, there is decreased contrast agent opacification of the kidneys and delayed contrast agent excretion. As renal function declines, calcifications can develop within the renal parenchyma. On MRI, the kidneys are enlarged and uniformly increased in signal intensity on T2-weighted images, with small, T2-hyperintense foci representing small parenchymal cysts. T1-weighted images demonstrate uniformly decreased signal intensity.

Acute Tubular Necrosis

Clinical Features

Acute tubular necrosis (ATN) is a common clinical problem, accounting for 45% of cases of acute kidney injury in the hospital setting.[11] ATN is characterized by an acute increase in serum creatinine of greater than 0.5 mg/dL/day from the patient's baseline, 1-2 days after exposure to a nephrotoxic agent or an episode of hypoperfusion. Common causes of ATN include renal hypoperfusion (because of blood loss, hypotension, or sepsis), major surgery, rhabdomyolysis, or exposure to nephrotoxic agents (such as certain chemotherapeutic agents, some antibiotics and antifungals, and iodinated contrast agents).

Pathology

An ATN is caused by the death of epithelial tubular cells, either because of exposure to a toxin or from ischemia. Gross examination of the kidney in patients with ATN demonstrates heavy swelling with a pale cortex and hyperemic medulla. The appearance of affected cells and debris within tubules may be suggestive of the etiology of the toxic insult. For example, the presence of clear crystals is suggestive of indinavir toxicity in patients who have been exposed to the drug.[12]

Radiologic Findings

Sonographic appearance of the kidneys in the presence of ATN is variable and depends on the underlying cause. For ischemic ATN, ultrasound is commonly normal. In patients with nephrotoxic ATN, the kidneys are variable in echogenicity with cortical hyperechogenicity

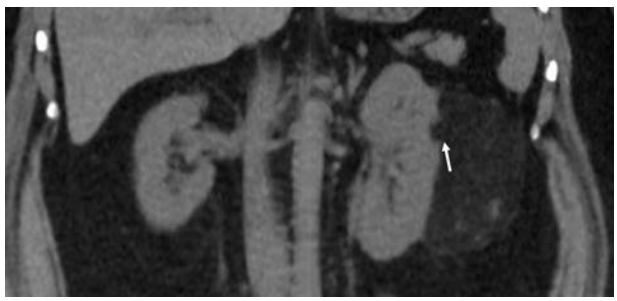

Fig. 5. Angiomyolipoma. Coronal unenhanced CT shows a fat density mass located within the perirenal space with extension into the renal parenchyma (arrow).

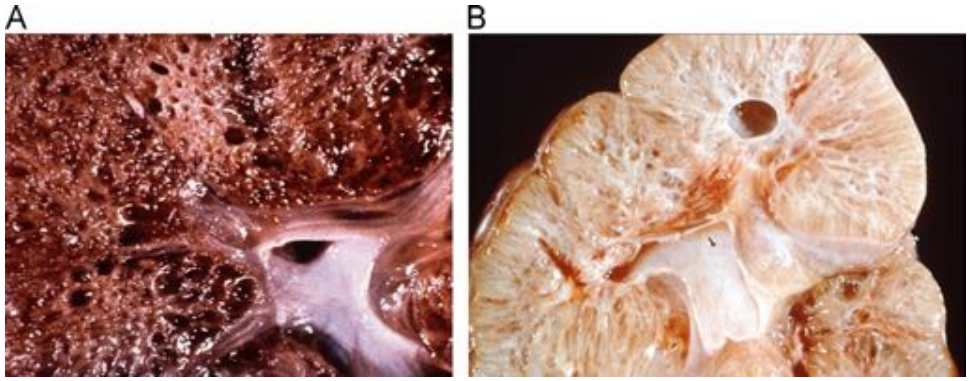

Fig. 6. Autosomal recessive polycystic kidney disease. Cut gross specimens from 2 different patients show innumerable cysts replacing the renal cortex and medulla (A) with loss of corticomedullary differentiation (B). (Color version of figure is available online.)

and preservation of corticomedullary differentiation being the most common appearance. Unenhanced CT may demonstrate normal renal parenchyma without obvious abnormality. In patients where iodinated contrast agent has served as a nephrotoxin, persistent nephrograms may be visualized on radiographs or CT performed up to 24 hours after contrast agent administration (Fig 9). Renal scintigraphy demonstrates normal blood flow and cortical accumulation of radiotracer, with a persistent nephrogenic phase and a delayed excretory phase on renogram (Fig 10).

Localized Cystic Renal Disease

Clinical Features

Localized cystic renal disease (LCRD) is a rare, benign, nonneoplastic proliferation of cysts within a normally functioning kidney. Correct diagnosis is critical, as this lesion may be confused with RCC, multicystic dysplastic kidney (MCDK), and ADPKD, although no genetic predisposition or association with increased risk of RCC, pseudoaneurysm, or cardiac valve defects has been associated with LCRD. In addition, there is no evidence of increased risk of renal failure in patients with LCRD.

Pathology

The pathophysiology of LCRD is unknown, as few cases are reported in the literature. Gross pathologic evaluation reveals unencapsulated, multicystic lesions of various sizes and extent, separated by renal parenchyma, which may be normal or atrophied (Fig 11). Cysts often contain clear, yellow fluid, but for this diagnosis, no evidence of papillary protrusions or tumor formation should be identified.[13]

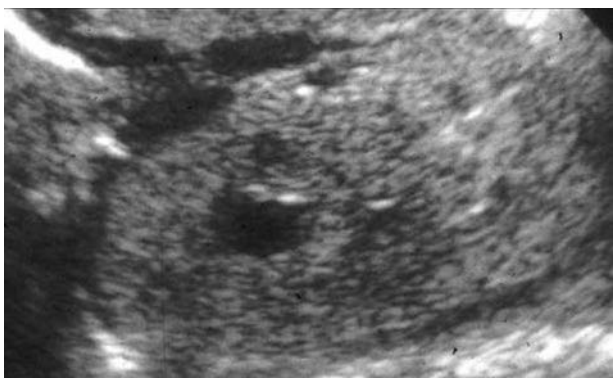

Fig. 7. Autosomal recessive polycystic kidney disease. Sagittal ultrasound image shows an enlarged, diffusely hyperechoic kidney with a thin hypoechoic cortex.

Radiologic Findings

LCRD is most commonly unilateral, with varying extent of renal involvement. Diffuse renal involvement is rare and could be confused with ADPKD. On ultrasound, cystic lesions are anechoic with thin, barely perceptible walls. The interspersed normal renal parenchyma may give the appearance of a multiseptated mass. CT reveals collections of nonencapsulated, nonenhancing cysts which most commonly measure at water density, although cases of hyperdense cysts have been reported, possibly representing previous trauma[13] (Fig 12). An MRI shows multiple cysts, the most of which should have simple fluid characteristics on all sequences. Intervening renal parenchyma, if normal, should have normal enhancement on both CT and MRI, whereas cysts should demonstrate no internal enhancement. If intracystic enhancement is noted, cystic RCC should be considered.

Multicystic Dysplastic Kidney

Clinical Features

Unilateral MCDK has an estimated incidence of 1 in every 4300 live births and has a slight male predominance.[14] MCDK is characterized by renal malformation (most commonly involving the entire kidney, although focal MCDK has been described), which results in renal dysfunction. MCDK is commonly diagnosed prenatally during second trimester fetal sonography.

Pathology

The pathophysiology of MCDK is poorly understood, as most morphologic studies of this condition have been performed on postnatally resected kidneys, which demonstrate severely

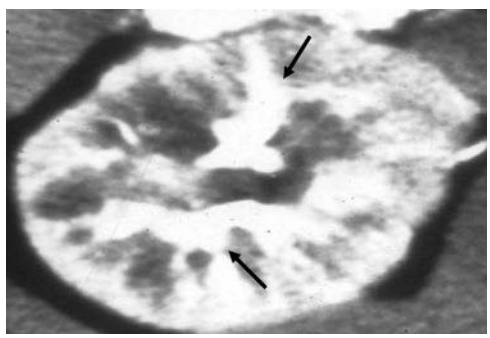

Fig. 8. Autosomal recessive polycystic kidney disease. Axial contrast-enhanced CT image shows a striated pattern of renal contrast agent excretion due to accumulation of contrast agent within dilated tubules (arrows).

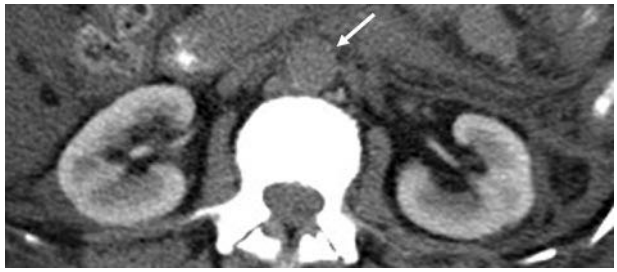

Fig. 9. Acute tubular necrosis. Axial unenhanced CT image shows bilateral persistent nephrograms in the absence of intraarterial contrast agent (arrow).

distorted architecture. A study performed on two fetal kidneys diagnosed with MCDK suggests that an intrinsic abnormality in the branching morphogenesis of the ureteric duct is responsible for disruption of normal nephrogenesis.[15] Gross pathology reveals severely distorted kidneys which contain variably-sized noncommunicating cysts. The renal pelvis is often atretic, or may demonstrate ureteropelvic junction obstruction (Fig 13).

Radiologic Findings

Prenatal and postnatal ultrasound reveals a multicystic mass within the affected renal fossa. Cysts are usually anechoic, thin walled, and vary widely in size. Occasionally, internal echoes may be present within cysts, representing internal debris. Residual atrophic renal parenchyma is hyperechoic due to replacement by fibrosis. Renal vessels are usually not visualized, with renal flow unidentifiable on the affected side (Fig 14). On CT and MR, a lobular multicystic mass composed of simple or minimally complicated cysts replaces the normal renal parenchyma. Some of these cysts may have developed wall calcifications, which are best seen on CT. With contrast, there is absent or minimal enhancement of the atrophic renal parenchyma on the affected side, with no evidence of contrast agent excretion. Radiographs may demonstrate a partially calcified, cystic mass with absent pyelogram if intravenous pyelography (IVP) is performed (Fig 15).

Multilocular Cystic RCC

Clinical Features

Multilocular cystic RCC (MCRCC) is a rare variant of clear cell carcinoma, which is estimated to comprise 1%-2% of all renal tumors.[16] The true incidence of this tumor is unknown, as diagnostic criteria were not defined by the World Health Organization until 2004.[17] MCRCC has a 3:1 male preponderance.[18]

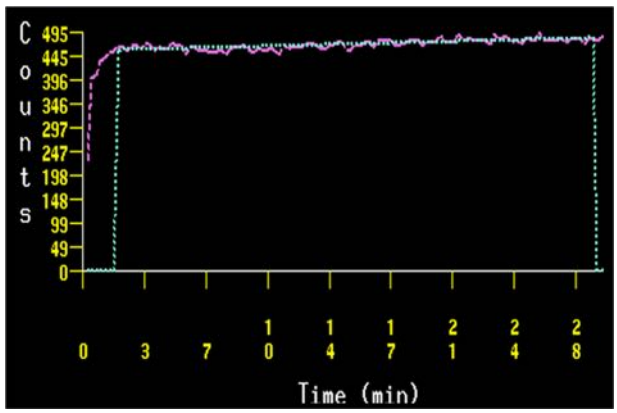

Fig. 10. Acute tubular necrosis. Renogram curve from renal scintigraphy using ^{99m}Tc-MAG$_3$ shows a prolonged nephrogenic phase. (Color version of figure is available online.)

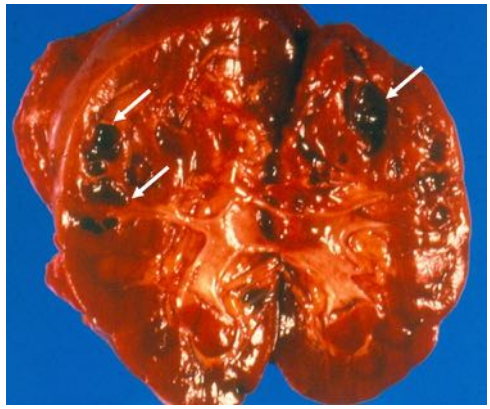

Fig. 11. Localized cystic renal disease. Cut gross specimen shows multiple unencapsulated cystic lesions separated by normal renal parenchyma which are localized to the renal upper pole (arrows). (Color version of figure is available online.)

Pathology

Gross pathologic assessment of MCRCC reveals well-circumscribed nodules composed entirely of noncommunicating cysts, separated by thick, irregular fibrous septa, which may contain calcification (Fig 16). There may be some limited yellowish solid present, without evidence of expansile nodules of clear cells within the septa or tumor necrosis.[19]

Radiologic Findings

Ultrasound shows a well-defined, multilocular mass composed of multiple cysts, which may vary in size and are separated by multiple septations. These septations may be nodular or demonstrate internal calcifications. Intracystic fluid is most commonly anechoic, but may be hyperechoic because of internal debris. CT reveals a well-defined multilocular cystic mass with thick, enhancing septa and enhancing solid components (which should compose less than 10% of the lesion)[20] (Fig 17). These findings may be suggestive of MCRCC, although not diagnostic, allowing for the potential selection of nephron-sparing surgery over nephrectomy.

Multilocular Cystic Nephroma

Clinical Features

Multilocular cystic nephroma (MLCN) is a benign neoplasm of the kidney, which demonstrates a bimodal age distribution, with peak incidence occurring at 2-4 years of age (infantile MLCN) and in the fourth through sixth decades (adult MLCN). There is a male

Fig. 12. Localized cystic renal disease. Axial-enhanced CT image in the excretory phase shows nonencapsulated discreet renal cysts (arrows) within the left kidney. Cysts are separated by normal renal tissue. The right kidney is normal.

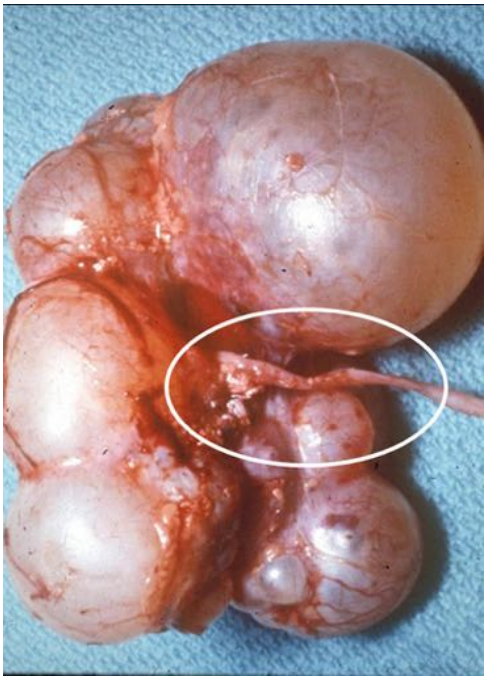

Fig. 13. Multicystic dysplastic kidney. Gross specimen shows multiple noncommunicating cysts with an atretic renal pelvis and ureter (circle). (Color version of figure is available online.)

predominance in infantile MLCN, with a 3:1 male-to-female ratio, which reverses to a female predominance in adult MLCN, which has a 1:8 male-to-female ratio.[21] The MLCN is considered to be a benign tumor which does not metastasize. Local recurrence is rare with only four reports of recurrent MLCN in the greater than 200 cases present in the literature.

Pathology

Gross assessment of MLCN shows a multiloculated, well-circumscribed mass surrounded by a thick fibrous capsule, which may have a nodular surface. When segmented, the mass demonstrates multiple non-communicating thin-walled cysts of differing sizes, which are often filled with clear fluid (Fig 18). No papillary projections or solid components should be identified within these cysts.

Radiologic Findings

On ultrasound, a multicystic tumor with thin septa is observed, which may have thin calcifications separating anechoic cystic

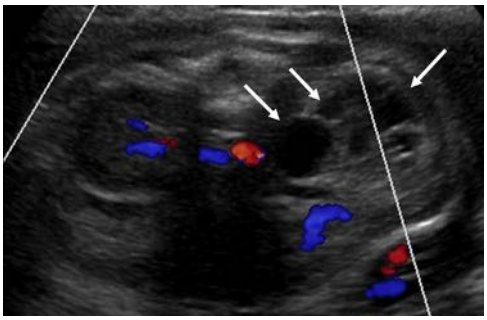

Fig. 14. Multicystic dysplastic kidney. Axial prenatal ultrasound performed during the second trimester demonstrates replacement of the normal renal parenchymal with multiple cysts (arrows). No vascular flow is visualized within the left kidney. The right kidney is normal. (Color version of figure is available online.)

Fig. 15. Multicystic dysplastic kidney. AP abdominal radiograph from an intravenous pyelogram shows calcified cystic lesions in the expected location of the left renal fossa (arrows). The left pyelogram is absent. A normal right pyelogram is also seen. AP, anteroposterior.

spaces. On CT imaging, a well-circumscribed, multiseptated mass with multiple water density cysts is seen (Fig 19). On MRI, cystic lesions follow simple fluid signal characteristics on all sequences. The thick surrounding fibrous capsule and internal septa are low in signal intensity on both T1-weighted and T2-weighted images. If contrast agent is administered, on CT or MRI, the septa demonstrates enhancement but no solid enhancing components should be present. Lack of hemorrhage into the tumor or perinephric space and herniation of the mass into the renal pelvis are classic findings of MLCN.

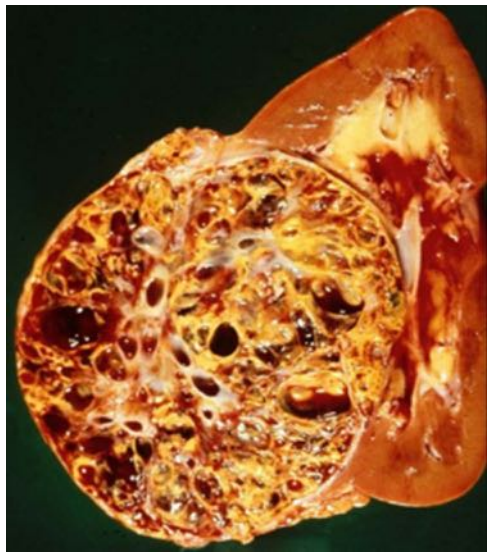

Fig. 16. Multilocular cystic renal cell carcinoma. Cut gross specimen shows an encapsulated mass composed of multiple non-communicating cysts separated by thick and irregular septa. (Color version of figure is available online.)

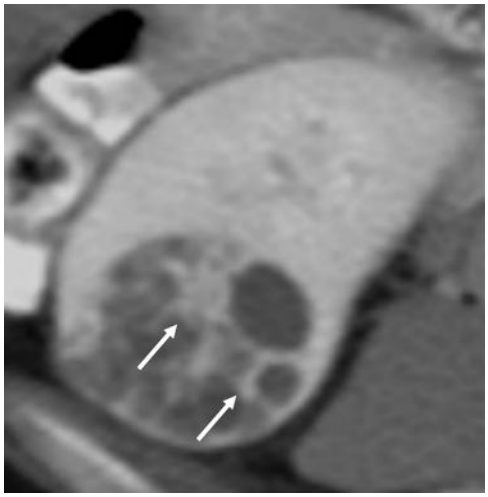

Fig. 17. Multilocular cystic renal cell carcinoma. Axial-enhanced CT image from the same patient as FIG 16 shows an encapsulated, multicystic lesion with thick, irregular, and enhancing septa (arrows).

Medullary Sponge Kidney

Clinical Features

Medullary sponge kidney (MSK) is a congenital disorder, affecting approximately 12% of patients with calcium nephrolithiasis.[22] Definitive diagnosis can be made with IVP or enhanced CT assessment of patients with renal dysfunction, nephrolithiasis, or nephrocalcinosis.

Pathology

MSK is believed to be caused by a developmental disruption of the ureteric bud–metanephric mesenchyme interface, leading to ectasia and cystic dilatation of the intrapapillary and intrapyramidal collecting ducts. Although commonly sporadic, familial clustering of MSK has been identified, as it has evidence of autosomal dominant transmission with variable penetrance.[23] Gross pathologic evaluation demonstrates normal-sized kidneys with multiple small cysts within the medullary pyramids and papillae, consistent with dilated collecting tubules. This gives a sponge-like appearance to the renal medulla (Fig 20).

Fig. 18. Multilocular cystic nephroma. Cut gross specimen shows a mass composed of non-communicating cysts with a thick, fibrous capsule. (Color version of figure is available online.)

Fig. 19. Multilocular cystic nephroma. Axial-enhanced CT image shows a mass composed of multiple simple cysts separated by thin septa, which demonstrate minimal enhancement. The mass extends into the renal pelvis.

Radiologic Findings

Radiographic diagnosis of MSK can only be performed with IVP or CT urography, as ultrasound and MRI are too low in spatial resolution for the identification of tubular ectasia. On ultrasound, MSK may be suggested if nephrocalcinosis is identified as hyperechoic foci with acoustic shadowing located within medullary pyramids (Fig 21). Unenhanced CT may reveal medullary nephrocalcinosis, with or without urolithiasis. If there is ureteral obstruction by nephrolithiasis, hydronephrosis may also be identified. On CT urography, dilated tubules within the medullary pyramids retain contrast agent. IVP shows linear or beaded densities of contrast agent accumulation within dilated ducts giving the classic “paintbrush” appearance of MSK (Fig 22).

Paroxysmal Nocturnal Hemoglobinuria

Clinical Features

Paroxysmal nocturnal hemoglobinuria (PNH) is a rare disorder with a reported symptomatic incidence of 1-10 cases per million people.[24] PNH occurs equally in males and females even though it is associated with a mutation of the X chromosome.

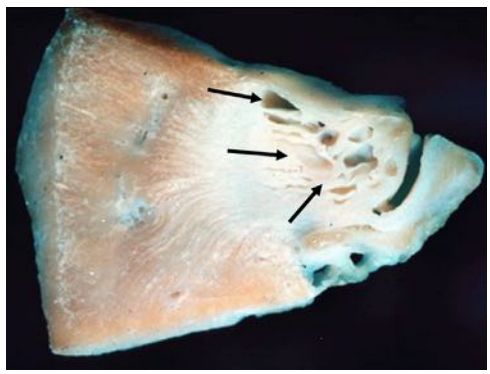

Fig. 20. Medullary sponge kidney. Cut gross specimen shows dilated collecting tubules (arrows) within the renal medulla. (Color version of figure is available online.)

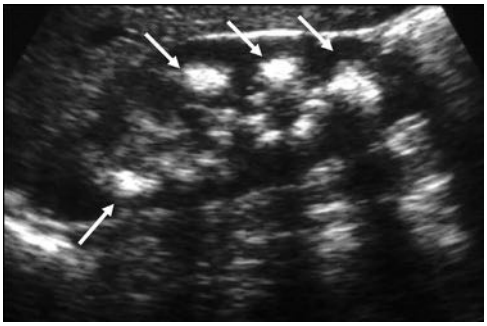

Fig. 21. Medullary sponge kidney. Sagittal ultrasound image shows shadowing hyperechoic foci (arrows) within the renal medulla, which are consistent with nephrocalcinosis.

Pathology

The PNH is caused by defective assembly of a glycolipid, glycosyl phosphatidylinositol, which is present on the surface of blood cells. This abnormality results in reduced cell protection against the complements system, leading to cell destruction. Although red blood cells, white blood cells, and platelets are all affected by this abnormality, red blood cells are most vulnerable; hemolysis is the predominant disorder in these patients. Chronic filtration of hemoglobin in these patients results in hemosiderin position within the renal cortex, secondary to heme transport molecules, which are located within the proximal tubules. On gross pathology, the bilateral kidneys are enlarged and demonstrate cortical thinning and interstitial scarring.

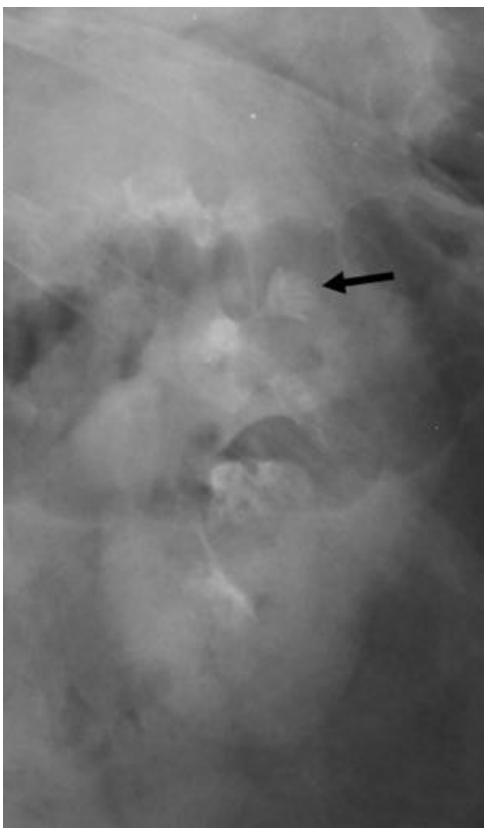

Fig. 22. Medullary sponge kidney. Frontal radiograph from an intravenous pyelogram shows extracalyceal contrast agent within dilated medullary tubules (arrows) giving the classic "paintbrush" appearance of MSK.

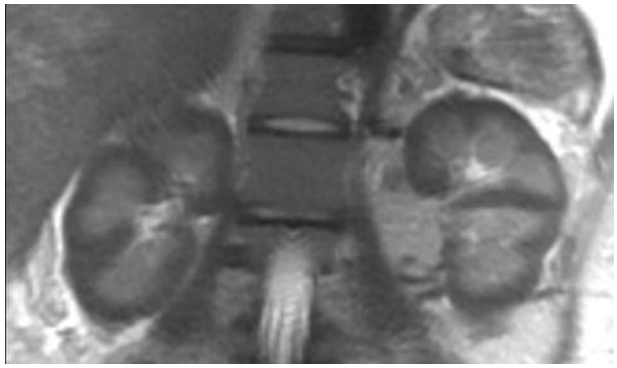

Fig. 23. Paroxysmal nocturnal hemoglobinuria. Coronal T2-weighted MRI image shows hypointense renal cortices relative to the normal renal medulla.

Radiologic Findings

There are no characteristic findings of PNH on radiographs or ultrasound. Unenhanced CT reveals increased attenuation of the renal cortex relative to the renal medulla due to hemosiderin deposition. MRI, which is the most sensitive imaging modality for evaluation of renal involvement with PNH, shows hypointense signal of the renal cortex relative to the renal medulla on T1-weighted, T2-weighted, and T2*-weighted images, owing to susceptibility artifact from ferric iron deposition (Fig 23). If contrast agent is administered on CT or MRI, renal function should be preserved and no specific abnormality relating to PNH is identified.

Renal Papillary Necrosis

Clinical Features

Renal papillary necrosis (RPN) is a pathologic entity resulting from a wide range of renal insults, including ischemia and nephrotoxic agents. The most common underlying etiologies are diabetes mellitus, analgesic nephropathy, sickle cell anemia, and infection (such as tuberculosis and pyelonephritis).

Pathology

RPN is the consequence of ischemic changes involving the renal papilla, which may be caused by direct occlusion of renal vessels (as seen in sickle cell anemia), compression of renal vasculature (as seen with inflammatory changes in pyelonephritis), or vasculitis (as seen with diabetes mellitus). If perfusion is not restored, irreversible lobar infarcts may result, causing complete or partial necrosis of the renal papilla. Renal papilla may slough, leaving cavities that communicate with the renal collecting system and create potential sites of abnormal contrast agent collection. On gross pathology, cortical atrophy is seen, with papilla in various stages of necrosis and sloughing (Fig 24).

Radiologic Findings

Sonography in the early stages of RPN may show echogenic rings with surrounding fluid within the renal medulla, representing necrotic papilla. This may give the appearance of pelvicalyceal dilatation. In late stages of RPN, there may be multiple cystic cavities within the medulla, and visible blunting of the calyces. Hyperechoic debris may be present within the collecting system, representing the sloughed papilla. Unenhanced CT is often normal in early RPN. In late or chronic RPN, the kidneys may be atrophic and scarred, with foci of medullary calcification. Enhanced CT

Fig. 24. Renal papillary necrosis. Cut gross specimen shows hemorrhagic renal papilla (arrow). (Color version of figure is available online.)

shows areas of decreased enhancement in the medullary tip, consistent with early papillary necrosis. The most sensitive modalities for the diagnosis of RPN are CT urography and IVP, both of which show extracalyceal contrast agent within the renal medulla and clubbed calyxes. Filling defects within the renal pelvis and ureter may represent sloughed papilla. Many signs have been described that detail the appearance of papillary necrosis, these include the "lobster claw" and "goblet" signs which correspond to contrast agent extending around a necrotic papilla, and the "ball-on-tee" sign which corresponds to extracalyceal contrast agent from a sloughed papilla (Fig 25).

Transitional Cell Carcinoma

Clinical Features

Renal pelvis and ureteral tumors account for approximately 10% all renal tumors with renal transitional cell carcinoma (TCC) representing 90% of these.[25] Renal TCC has a male predominance, with males affected 2 times more commonly than women do.[26] A high percentage of patients with renal TCC also concurrently have TCC within the bladder, which may be either synchronous (13%) or metachronous (24%-31%).[27] Owing to this high rate of concurrent bladder TCC, continued surveillance in patients who have undergone nephroureterectomy for TCC is recommended with ureteroscopy and CT or MRI every 6 months.[28]

Pathology

Renal TCC is histologically identical to bladder TCC and is thought to be at least partially caused by exposure of the urothelium to potential carcinogens present within urine, which may account for the multifocality and bilaterality of these tumors. On gross pathology, renal TCC appears as a white or tan polypoid mass located within and filling the renal pelvis, calyces or both. There may be visible gross invasion of the adjacent renal parenchyma.

Radiologic Findings

Sonographic assessment may reveal a mass within the renal collecting system (which can be difficult to differentiate from a blood clot if internal vascularity is not identified on color Doppler images) or eccentric thickening of the pelvic or calyceal urothelium. On unenhanced CT, renal mass may appear isodense or slightly hyperdense relative to urine and renal parenchyma. Enhanced CT may show focal pelvic wall thickening, or a hypoattenuating mass either extending from the renal urothelium or invading into the renal parenchyma (Fig 26). Often, this hypoattenuating mass is best seen on delayed images or CT urography, where contrast agent may be seen surrounding the hypodense mass. On MRI, which is less sensitive than CT, renal TCC is isointense or hypointense relative to renal parenchyma on T1-weighted images, and isointense to hyperintense to renal parenchyma on T2-weighted images. Enhancement characteristics are variable and may demonstrate a filling defect within the renal collecting system if magnetic resonance urography is performed. Rarely, there may be hydronephrosis due to ureteral pelvic junction obstruction by tumor, although hydronephrosis is more common with ureteral TCC.

Xanthogranulomatous Pyelonephritis

Clinical Features

Xanthogranulomatous pyelonephritis (XGPN) is a chronic infective pyelonephritis characterized by extensive destruction of the involved kidney, which is estimated to occur in 1% of renal infections.[29] Associated renal failure is rarely identified because of compensatory functioning of the contralateral kidney.

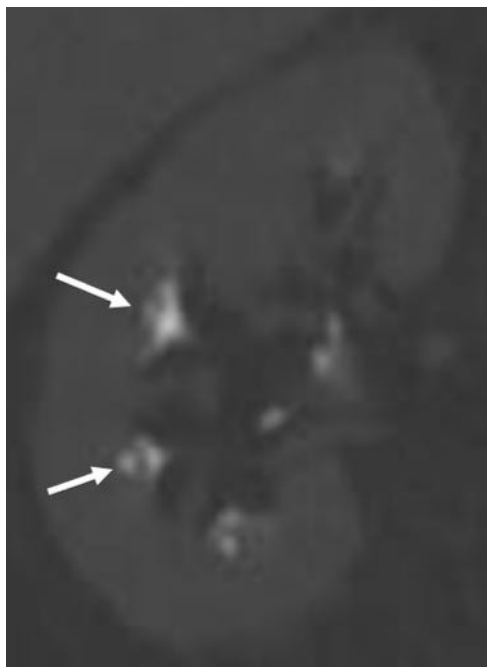

Fig. 25. Renal papillary necrosis. Coronal image from CT urography shows extracalyceal contrast agent giving a "ball-on-tee" appearance (arrows).

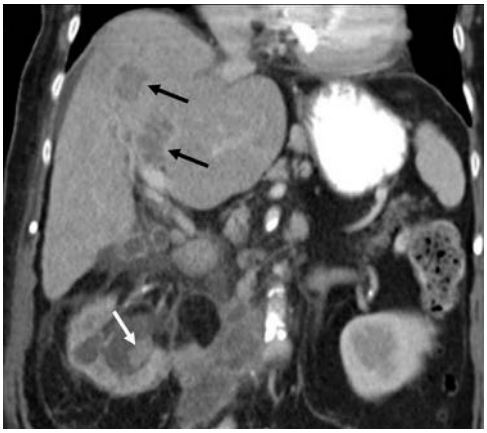

Fig. 26. Transitional cell carcinoma. Coronal-enhanced CT image shows an enhancing mass within the right renal pelvis (white arrow), which is dilated. Hypoattenuating metastases are present within the liver (black arrows).

Fig. 27. Xanthogranulomatous pyelonephritis. Cut gross specimen demonstrates an enlarged kidney with replacement of the normal renal parenchyma by areas of necrosis and yellow nodules (arrows). A staghorn calculus is present within the pelvis (circle). (Color version of figure is available online.)

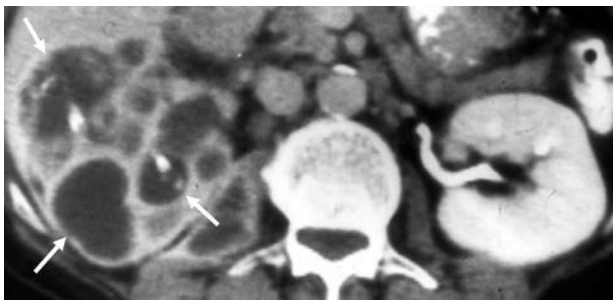

Fig. 28. Xanthogranulomatous pyelonephritis. Axial-enhanced CT image shows multiple low attenuation, rim-enhancing masses (arrows) replacing the parenchyma of the right kidney. The left kidney is normal in appearance.

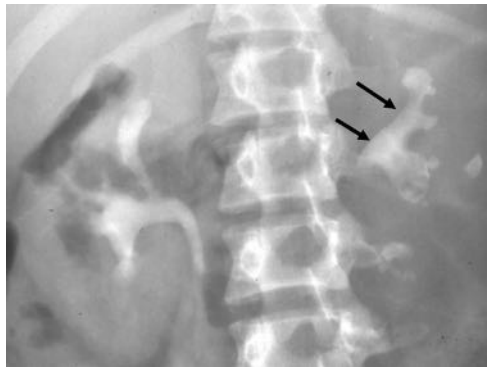

Fig. 29. Xanthogranulomatous pyelonephritis. AP radiograph from an intravenous pyelogram shows a staghorn calculus (arrows) in the region of the left renal fossa with an absent left sided nephrogram. Right nephrogram is normal. AP, anteroposterior.

Pathology

The underlying etiology of xanthogranulomatous pyelonephritis is unknown, although urinary tract obstruction and infection have been identified as key underlying factors. On gross pathology, the affected kidney is enlarged, as are the renal pelvis and calyces. Staghorn calculus and pyonephrosis are often also present. Upon segmentation, replacement of the normal corticomedullary tissue with orange-yellow nodular inflammatory lesions and areas of necrosis and abscess formation (Fig 27) may be seen. Although in rare cases involvement may be focal, most commonly there is involvement of the entire kidney.

Radiologic Findings

Sonographic assessment shows an enlarged kidney, with loss of corticomedullary differentiation and multiple anechoic or hypoechoic masses replacing the normal renal parenchyma. These lesions may represent dilated calyces, abscesses, or granulomas. The renal pelvis is contracted owing to fibrosis and may have a hyperechoic central mass representing a staghorn calculus. Enhanced CT and MRI reveal multiple cystic lesions replacing the normal renal parenchyma, which is hypoattenuating on CT (Fig 28) and T1 hypointense and T2 hyperintense on MRI. If present, solid components within these predominantly cystic lesions demonstrate loss of signal on fat-suppressed images, because of internal lipid content. Staghorn calculus appears hyperdense on CT but hypointense on all MRI sequences. IVP reveals a staghorn calculus in the expected location of the renal pelvis, with an absent ipsilateral pyelogram (Fig 29).

Conclusion

Like many other aspects of medicine, renal pathology has been shortened to multiple confusing abbreviations. This article sought to lessen some of this confusion by delving into the different radiographic and pathologic appearances of these entities and to explain the underlying pathophysiology. By understanding these intricacies, physicians should be better able to distinguish these entities, decreasing confusion in the interactions between radiologists and clinicians.

References

1. Berland Y, Dussol B. Nephrologie Pour L'interne. ed 1. Paris: Elsevier Masson; 2000.

2. Hassan I, Junejo AM, Dawani ML. Etiology and outcome of acute renal failure in pregnancy. J Coll Physicians Surg Pak 2009;19:714–7.
3. Hateboer N, v Dijk MA, Bogdanova N, et al. Comparison of phenotypes of polycystic kidney disease types 1 and 2. European PKD1-PKD2 Study Group. Lancet 1999;353:103–7.
4. Halvorson CR, Bremmer MS, Jacobs SC. Polycystic kidney disease: Inheritance, pathophysiology prognosis, and treatment. Int J Nephrol Renovasc Dis 2010;3:69–83.
5. Keith DS, Torres VE, King BF, et al. Renal cell carcinoma in autosomal dominant polycystic kidney disease. J Am Soc Nephrol 1994;4:1661–9.
6. Rule AD, Sasiwimonphan K, Lieske JC, et al. Characteristics of renal cystic and solid lesions based on contrast-enhanced computed tomography of potential kidney donors. Am J Kidney Dis 2012;59:611–8.
7. El Sayed Esheba G, El Sayed Esheba N. Angiomyolipoma of the kidney: Clinicopathological and immunohistochemical study. J Egypt Natl Canc Inst 2013;25:125–34.
8. Meaglia JP, Schmidt JD. Natural history of an adrenal myelolipoma. J Urol 1992;147:1089–90.
9. Guay-Woodford LM, Bissler JJ, Braun MC, et al. Consensus expert recommendations for the diagnosis and management of autosomal recessive polycystic kidney disease: Report of an international conference. J Pediatr 2014;165:611–7.
10. Menezes LF, Cai Y, Nagasawa Y, et al. Polyductin, the PKHD1 gene product, comprises isoforms expressed in plasma membrane, primary cilium, and cytoplasm. Kidney Int 2004;66:1345–55.
11. Hou SH, Bushinsky DA, Wish JB, et al. Hospital-acquired renal insufficiency: A prospective study. Am J Med 1983;74:243–8.
12. Wyatt CM, Morgello S, Katz-Malamed R, et al. The spectrum of kidney disease in patients with AIDS in the era of antiretroviral therapy. Kidney Int 2009;75:428–34.
13. Slywotzky CM, Bosniak MA. Localized cystic disease of the kidney. Am J Roentgenol 2001;176:843–9.
14. Schreuder MF, Westland R, van Wijk JA. Unilateral multicystic dysplastic kidney: A meta-analysis of observational studies on the incidence, associated urinary tract malformations and the contralateral kidney. Nephrol Dial Transplant 2009;24:1810–8.
15. Matsell DG, Bennett T, Goodyer P, et al. The pathogenesis of multicystic dysplastic kidney disease: Insights from the study of fetal kidneys. Lab Invest 1996;74:883–93.
16. Han KR, Janzen NK, McWhorter VC, et al. Cystic renal cell carcinoma: Biology and clinical behavior. Urol Oncol 2004;22:410–4.
17. Suzigan S, Lopez-Beltran A, Montironi R, et al. Multilocular cystic renal cell carcinoma. Am J Clin Pathol 2006;125:217–22.
18. Chowdhury AR, Chakraborty D, Bhattacharya P, et al. Multilocular cystic renal cell carcinoma a diagnostic dilemma: A case report in a 30-year-old woman. Urol Ann 2013;5:119–21.
19. Wahal SP, Mardi K. Multilocular cystic renal cell carcinoma: A rare entity with review of literature. J Lab Physicians 2014;6:50–2.
20. Kim JC, Kim KH, Lee JW. CT and US findings of multilocular cystic renal cell carcinoma. Korean J Radiol 2000;1:104–9.
21. Castillo OA, Boyle ET Jr, Kramer SA. Multilocular cysts of kidney. A study of 29 patients and review of literature. Urology 1991;37:156–62.
22. Yagisawa T, Kobayashi C, Hayashi T, et al. Contributory metabolic factors in the development of nephrolithiasis in patients with medullary sponge kidney. Am J Kidney Dis 2001;37:1140–3.
23. Goldman SH, Walker SR, Merigan TC Jr, et al. Hereditary occurrence of cystic disease of the renal medulla. N Engl J Med 1966;274:984–92.
24. Borowitz MJ, Craig FE, Digiuseppe JA, et al. Guidelines for the diagnosis and monitoring of paroxysmal nocturnal hemoglobinuria and related disorders by flow cytometry. Cytometry B Clin Cytom 2010;78:211–30.
25. Siegel RL, Miller KD, Jemal A. Cancer statistics, 2015. CA Cancer J Clin 2015;65:5–29.
26. Raman JD, Messer J, Sielatycki JA, et al. Incidence and survival of patients with carcinoma of the ureter and renal pelvis in the USA, 1973-2005. BJU Int 2011;107:1059–64.
27. Yousem DM, Gatewood OM, Goldman SM, et al. Synchronous and metachronous transitional cell carcinoma of the urinary tract: Prevalence, incidence, and radiographic detection. Radiology 1988;167:613–8.
28. Kang CH, Yu TJ, Hsieh HH, et al. The development of bladder tumors and contralateral upper urinary tract tumors after primary transitional cell carcinoma of the upper urinary tract. Cancer 2003;98:1620–6.
29. Siddappa S, Ramprasad K, MuddeGowda MK. Xanthogranulomatous pyelonephritis: A retrospective review of 16 cases. Korean J Urol 2011;52:421–4.